Comparison of Levant differentiator and GPI observer for the position/force control of robotic manipulator interacting with unknown rigid surfaces

Lauro Fernando Vázquez–Alberto *

* *Departamento de Control y Robótica. División de Ingeniería Eléctrica de la Facultad de Ingeniería. Universidad Nacional Autónoma de México. Apdo. Postal 70–256, México, D. F., 04510, México. raztek_lion@hotmail.com*

Abstract: The problem of hybrid position/force control over rigid surfaces when only joint position and force measurements are available is considered. To achieve position tracking in this scheme it is commonly assumed that the contact force on the robot and the angular velocity are measured. Nevertheless, in some applications it is convenient to remove sensors for a variety of reasons: to reduce costs, the weight of the robot, the size, etc. In this work, a Levant–differentiator approach is used to estimate velocity in order to achieve position tracking for the non–delayed scenario but with force measurement. To achieve this objective, a comparison with a dynamic extension and a high–gain observer were employed, which are known in the literature as Generalized Proportional Integral (GPI) observers. The GPI observer allows, besides simultaneous estimation of robot joint velocity and the contact force over the environment. In other words, the proposed algorithm achieves movement of the robot over the surface and simultaneous application of a force desired, while at the same time it performs an estimation of the velocity and force signals. There are some advantages in using the Levant differentiator such as improved tracking position without the knowledge of the robot dynamic model for implementation.

Keywords: Robotic manipulators, Levant differentiator, GPI.

1. INTRODUCTION

Many applications involving a robotic manipulator require its interaction with the environment. In such a case, it becomes necessary to control not only the motion of the manipulator but also the interaction force with the environment. There are basically two approaches to deal with the motion and force control problem: the direct and indirect force control. In the later the position and force control are achieved by establishing the desired impedance between the end-effector and the environment. Impedance and Compliance controllers belong to this category. On the other hand, in the direct force approach the task is achieved by taking into account an explicit force feedback, e.g. hybrid control. For the contact with rigid surfaces some approaches have been developed based on linear observers (Hacksel and Salcudean, 1994), (Martínez-Rosas et al., 2006), nonlinear observers based on PID control (Arteaga-Pérez et al., 2013), and GPI observers (Gutiérrez-Giles and Arteaga-Pérez, 2014). Most of the cases, force observes require a dynamic model of the robot. To overcome the unknown surface problem this can be considered as a hybrid system Shaft and Schumacher (2000). With the force measurement and the velocity estimation we can estimate the surface. A comparison between two different velocity estimator schemes is carried out, guaranteeing position and force tracking over a surface. Simulations results are presented to support the validity of the proposed approach. The first approach to deal with the motion and force control problem, and the main results are from Gutiérrez-Giles and Arteaga-Pérez (2016), Gutiérrez-Giles (2016), and with the position measurement and the Levant differentiator the latter velocity estimation is obtained to be used with the same control scheme.

Alternatively to the use of a controller *GPI* Gutiérrez-Giles and Arteaga-Pérez (2016), Gutiérrez-Giles (2016) the Levant differentiator can be used to estimate the velocity. To the best of the author knowledge there are no similar results for the problem treated here, i.e., using the Levant differentiator to estimate the velocity for the hybrid force/position control without velocity measurements and without a geometric description of the surface. Although the main idea is new to there are some differences and advantages in this work. The first difference is that no knowledge of the dynamic robot model is needed to implement the differentiator. Is not

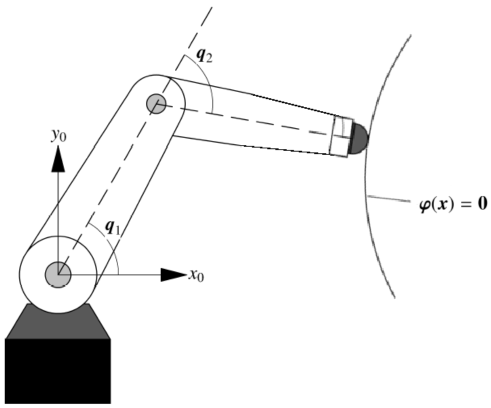

Fig. 1. Two link planar robot in contact with a surface.

compensating for robot dynamic uncertainties Jung and Hsia (2000), the use of the robot dynamic model is not required, just the joints position, for simulations results is required but for implementation is not necessary. A second distinction of this work is that the proposed differentiator is designed to use a minimal computing resources, which is an important practical advantage.

The paper is organized as follows: in Section 2 the mathematical model of the systems is given and some useful properties as well. In Section 3 is presented the main result, that is, the observer and controller design. A numerical simulation to illustrate the approach is presented in Section 4. Finally, some conclusions are given in Section 5.

2. MATHEMATICAL MODEL AND PROPERTIES

Consider a n–degrees of freedom manipulator in contact with a rigid surface Figure 1. Let $\boldsymbol{q} \in \Re^n$ be the vector of generalized coordinates and $\boldsymbol{\tau} \in \Re^n$ the vector of input torques. The corresponding dynamic model is given by

$$\boldsymbol{H}(\boldsymbol{q})\ddot{\boldsymbol{q}} + \boldsymbol{C}(\boldsymbol{q}, \dot{q})\dot{\boldsymbol{q}} + \boldsymbol{D}\dot{\boldsymbol{q}} + \boldsymbol{g}(\boldsymbol{q}) = \boldsymbol{\tau} + \boldsymbol{J}_{\varphi}^{T}(\boldsymbol{q})\boldsymbol{\lambda} \qquad (1)$$

where, for the manipulator, $\boldsymbol{H} = \boldsymbol{H}(\boldsymbol{q}) \in \Re^{n\times n}$ is the inertia matrix, $\boldsymbol{C}\dot{\boldsymbol{q}} = \boldsymbol{C}(\boldsymbol{q}, \dot{\boldsymbol{q}})\dot{\boldsymbol{q}} \in \Re^n$ is the vector of centrifugal and Coriolis forces, $\boldsymbol{D} \in \Re^{n\times n}$ is a diagonal matrix of viscous friction coefficients, $\boldsymbol{g} = \boldsymbol{g}(\boldsymbol{q}) \in \Re^n$ is the vector of gravitational torques, $\boldsymbol{\tau} \in \Re^n$ is the vector of input torques, $\boldsymbol{\lambda} \in \Re^{n\times n}$ is the vector of Lagrange multipliers (physically represents the force exerted by the manipulator over the environment at the contact point), and $\boldsymbol{J}_{\varphi}^{T}(\boldsymbol{q}) \triangleq \frac{\partial \boldsymbol{\varphi}(q)}{\partial \boldsymbol{q}} \in \Re^n$ is the gradient of the m holonomic constrains, specified in terms of the generalized coordinates, defined by

$$\boldsymbol{\varphi}(\boldsymbol{q}) = 0 \qquad (2)$$

These constrains can also be defined in terms of the end effector coordinates $\boldsymbol{x} \in \Re^n$

$$\boldsymbol{\varphi}(\boldsymbol{x}) = 0 \qquad (3)$$

$$\boldsymbol{J}_{\varphi}(\boldsymbol{q}) = \boldsymbol{J}_{\varphi x}\boldsymbol{J}(\boldsymbol{q}) \qquad (4)$$

where $\boldsymbol{J}(\boldsymbol{q}) \in \Re^{n\times n}$ is the analytic Jacobian of the manipulator. Note that with a suitable normalization it can be done $\| \boldsymbol{J}_{\varphi x} \| = 1$. For simplicity, we assume that the robots have only revolute joints. In such case, for each manipulator, the following well–known properties hold (Arteaga-Pérez, 1998).

Property 2.1. The inertia matrix is symmetric, positive definite and fulfils $\lambda_{\rm h}\|\boldsymbol{x}\|^2 \leq \boldsymbol{x}^{\rm T}\boldsymbol{H}_i(\boldsymbol{q}_i)\boldsymbol{x} \leq \lambda_{\rm H}\|\boldsymbol{x}\|^2\,\forall \boldsymbol{x} \in \Re^n$, with $0 < \lambda_{\rm h} \leq \lambda_{\rm H} < \infty$. □

Property 2.2. With a proper definition of $\boldsymbol{C}_i(\boldsymbol{q}_i, \dot{\boldsymbol{q}}_i)$, the matrix $\dot{\boldsymbol{H}}_i - 2\boldsymbol{C}_i$ is skew–symmetric. □

Property 2.3. The vector $\boldsymbol{C}_i(\boldsymbol{q}_i, \dot{\boldsymbol{q}}_i)\dot{\boldsymbol{q}}_i$ fulfils $\boldsymbol{C}_i(\boldsymbol{q}_i, \boldsymbol{x})\boldsymbol{y} = \boldsymbol{C}_i(\boldsymbol{q}_i, \boldsymbol{y})\boldsymbol{x}\,, \forall \boldsymbol{x}, \boldsymbol{y} \in \Re^n$. □

3. OBSERVER AND CONTROLLER DESIGN

Let $\boldsymbol{q}_1 \triangleq \boldsymbol{q}$ and $\boldsymbol{q}_2 \triangleq \dot{\boldsymbol{q}}$. A state space representation of (1) is given by

$$\dot{\boldsymbol{q}}_1 = \boldsymbol{q}_2 \qquad (5)$$

$$\dot{\boldsymbol{q}}_2 = \boldsymbol{H}^{-1}\boldsymbol{q}_1\left(\boldsymbol{\tau} - \boldsymbol{N}(\boldsymbol{q}_1, \boldsymbol{q}_2)\right) + \boldsymbol{z}_1\,, \qquad (6)$$

where $\boldsymbol{N}(\boldsymbol{q}_1, \boldsymbol{q}_2) \triangleq \boldsymbol{C}(\boldsymbol{q}_1, \boldsymbol{q}_2)\boldsymbol{q}_2 + \boldsymbol{D}\boldsymbol{q}_2 + \boldsymbol{g}(\boldsymbol{q}_1)$ and $\boldsymbol{z}_1 \triangleq \boldsymbol{H}^{-1}(\boldsymbol{q}_1)\boldsymbol{J}_{\varphi}^{T}(\boldsymbol{q}_1)\boldsymbol{\lambda}$. One of the goals of the first scheme is to estimate the contact force $\boldsymbol{\lambda}$, contained in the variable $\boldsymbol{z}_1$, by taking into account the following (Sira-Ramírez et al., 2010).

Assumption 3.1. The vector $\boldsymbol{z}_1$ can be written as

$$\boldsymbol{z}_1(t) = \sum_{i=1}^{p} \boldsymbol{a}_i t^i + \boldsymbol{r}(t)\,, \qquad (7)$$

where $\boldsymbol{a}_i \in \Re^n, i = 1, \ldots, p$ is a vector of constant coefficients and $\boldsymbol{r}_i \in \Re^n$ is a residual term. □

Assumption 3.2. Each vector $\boldsymbol{z}_1$ and at least its first p time derivatives exist (Gutiérrez-Giles and Arteaga-Pérez, 2014). □

By taking into account Assumptions 3.1 and 3.2, an internal model for each time vector $\boldsymbol{z}_{1i}(t)$ can be written as

$$\dot{\boldsymbol{z}}_1 = \boldsymbol{z}_2 \qquad (8)$$

$$\dot{\boldsymbol{z}}_2 = \boldsymbol{z}_3 \qquad (9)$$

$$\vdots$$

$$\dot{\boldsymbol{z}}_{(p-1)} = \boldsymbol{z}_p \qquad (10)$$

$$\dot{\boldsymbol{z}}_p = \boldsymbol{r}^{(p)}(t)\,. \qquad (11)$$

3.1 Observers' design

To avoid the measurement of the joint–velocities for each manipulator and the contact force that the robot exerts over the environment, (Gutiérrez-Giles, 2016) propose the following linear high–gain observer

$$\dot{\hat{\boldsymbol{q}}}_1 = \hat{\boldsymbol{q}}_2 + \boldsymbol{\lambda}_{p+1}\tilde{\boldsymbol{q}}_1 \tag{12}$$

$$\dot{\hat{\boldsymbol{q}}}_2 = \boldsymbol{H}^{-1}\boldsymbol{q}_1\left(\boldsymbol{\tau} - \boldsymbol{N}(\boldsymbol{q}_1, \dot{\hat{\boldsymbol{q}}}_2)\right) + \hat{\boldsymbol{z}}_1 + \boldsymbol{\lambda}_p\tilde{\boldsymbol{q}}_1 \tag{13}$$

$$\dot{\hat{\boldsymbol{z}}}_1 = \hat{\boldsymbol{z}}_2 + \boldsymbol{\lambda}_{p-1}\tilde{\boldsymbol{q}}_1 \tag{14}$$

$$\dot{\hat{\boldsymbol{z}}}_2 = \hat{\boldsymbol{z}}_3 + \boldsymbol{\lambda}_{p-2}\tilde{\boldsymbol{q}}_1 \tag{15}$$

$$\vdots$$

$$\dot{\hat{\boldsymbol{z}}}_{(p-1)} = \hat{\boldsymbol{z}}_p + \boldsymbol{\lambda}_1\tilde{\boldsymbol{q}}_1 \tag{16}$$

$$\dot{\hat{\boldsymbol{z}}}_p = \boldsymbol{\lambda}_0\tilde{\boldsymbol{q}}_1\,, \tag{17}$$

where $\tilde{\boldsymbol{q}}_1 \triangleq \boldsymbol{q}_1 - \hat{\boldsymbol{q}}_1$, and $\hat{\boldsymbol{N}}(\boldsymbol{q}_1, \dot{\hat{\boldsymbol{q}}}_2) = \boldsymbol{C}(\boldsymbol{q}_1, \dot{\hat{\boldsymbol{q}}}_2)\hat{\boldsymbol{q}}_2 + \boldsymbol{D}\dot{\hat{\boldsymbol{q}}}_2 + \boldsymbol{g}(\boldsymbol{q}_1)$. Note that $\hat{\boldsymbol{q}}_2$ is imployed instead of $\boldsymbol{q}_2$ to avoid velocity measurements.

From (4) and (6) it follows

$$\boldsymbol{J}_{\varphi x}^{\boldsymbol{T}}\boldsymbol{\lambda} = \boldsymbol{J}^{-T}(\boldsymbol{q}_1)\boldsymbol{H}(\boldsymbol{q}_1)\boldsymbol{z}_1 \tag{18}$$

Therefore, an estimate of the contact force could be computed as

$$\hat{\boldsymbol{\lambda}} = \parallel \boldsymbol{J}_{\varphi x}^{\boldsymbol{T}}\boldsymbol{\lambda} \parallel = \parallel \boldsymbol{J}^{-T}(\boldsymbol{q}_1)\boldsymbol{H}(\boldsymbol{q}_1)\boldsymbol{z}_1 \parallel \tag{19}$$

because $\parallel \boldsymbol{J}_{\varphi x}^{\boldsymbol{T}} \parallel = 1$. Because it is assumed that the geometry of the constraint surface is not known, an online estimation of the gradient of this surface in workspace coordinates is proposed as

$$\dot{\hat{\boldsymbol{J}}}_{\varphi x}^{\boldsymbol{T}} = \left(\frac{\gamma}{\hat{\lambda} + \epsilon}\right)\hat{\boldsymbol{Q}}_x\boldsymbol{J}^{-T}(\boldsymbol{q}_1)\boldsymbol{H}(\boldsymbol{q}_1)\boldsymbol{z}_1 \tag{20}$$

where $\gamma > 0$ is a scalar adaptation gain, $\epsilon << \lambda$ is a (small) positive constant to avoid division by zero. Any r-sliding homogeneous controller can be complemented by an $(r-1)$th order differentiator producing an output-feedback controller. Given the bounded function $f(t)$ defined in the interval $[0, \infty]$, with unknown measurements but bounded and signal $f_0(t)$ unknown, to estimate $\dot{f}_0(t), \ddot{f}_0(t), ..., f_0^k(t)$ in real time the following differentiator is used (Levant, 2003). Any r-sliding homogeneous controller can be complemented by an $(r-1)$th order differentiator producing an output-feedback controller. The Levant differentiator is defined

$$\begin{aligned} \dot{z}_0 &= v_0, \\ v_0 &= -\lambda_k L^{1/(k+1)} \mid z_0 - f(t) \mid^{k/(k+1)} sign(z_0 - f(t)) \\ &\quad + z_1 \end{aligned} \tag{21}$$

$$\begin{aligned} \dot{z}_1 &= v_1, \\ v_1 &= -\lambda_k L^{1/k} \mid z_1 - v_0 \mid^{(k+1)/k} sign(z_1 - v_0) \\ &\quad + z_2 \end{aligned} \tag{22}$$

$$\vdots \tag{23}$$

$$\begin{aligned} \dot{z}_{k-1} &= v_{k-1}, \\ v_{k-1} &= -\lambda_1 L^{1/2} \mid z_{k-1} - v_{k-2} \mid^{1/2} sign(z_{k-1} - v_{k-2}) \\ &\quad + z_k \end{aligned} \tag{24}$$

$$\dot{z}_k = -\lambda_0 L sign(z_k - v_{k-1}) \tag{25}$$

To estimate the velocity required one of the options is to use a Levant third order differentiator.

$$v_0 = -2L \mid z_0 - f \mid^{\frac{2}{3}} sign(z_0 - f) + z1 \tag{26}$$

$$v_1 = -1.5L \mid z_1 - v_0 \mid^{\frac{1}{2}} sign(z_1 - v_0) + z2 \tag{27}$$

$$v_2 = -1.1L(z_2 - v_1) \tag{28}$$

$$\dot{z}_0 = v_0 \tag{29}$$

$$\dot{z}_1 = v_1 \tag{30}$$

$$\dot{z}_2 = v_2 \tag{31}$$

the gains for the Levant differentiator are defined in (Shtessel et al., 2014).

3.2 Controllers' design

To achieve position and force tracking (Gutiérrez-Giles and Arteaga-Pérez, 2016) propose the control law.

$$\begin{aligned} \boldsymbol{\tau} &= -\boldsymbol{K}_p\boldsymbol{e}_1 - \boldsymbol{K}_v(\hat{\boldsymbol{q}}_2 - \dot{\boldsymbol{q}}_d) \\ &\quad - \hat{\boldsymbol{Q}}\boldsymbol{K}_i\int_0^t \boldsymbol{e}_1 d\boldsymbol{\vartheta} - \hat{\boldsymbol{J}}_{\varphi}^{\boldsymbol{T}}\boldsymbol{\lambda}_d + \hat{\boldsymbol{J}}_{\varphi}^{+}\boldsymbol{k}_{Fi}\boldsymbol{\Delta}\bar{F} \end{aligned} \tag{32}$$

where $\boldsymbol{K}_p, \boldsymbol{K}_v, \boldsymbol{K}_i \in \mathbb{R}^{n \times n}$ are diagonal positive definite matrices of constant gains, $\boldsymbol{k}_{Fi} > 0$ is the integral force control gain $\boldsymbol{e}_1 \triangleq \boldsymbol{q}_1 - \boldsymbol{q}_d$ is the position tracking error, and

$$\hat{\boldsymbol{J}}_{\varphi}^{\boldsymbol{T}} \triangleq \boldsymbol{J}(\boldsymbol{q})\hat{\boldsymbol{J}}_{\varphi x}^{\boldsymbol{T}} \tag{33}$$

$$\hat{\boldsymbol{J}}_{\varphi}^{+} \triangleq \hat{\boldsymbol{J}}_{\varphi}^{\boldsymbol{T}}\left(\hat{\boldsymbol{J}}_{\varphi}\hat{\boldsymbol{J}}_{\varphi}^{\boldsymbol{T}}\right)^{-1} \tag{34}$$

$$\hat{\boldsymbol{Q}} \triangleq \boldsymbol{I} - \hat{\boldsymbol{J}}_{\varphi}^{+}\hat{\boldsymbol{J}}_{\varphi} \tag{35}$$

Also, it is defined

$$\boldsymbol{\Delta}\bar{\lambda} \triangleq \hat{\boldsymbol{\lambda}} - \boldsymbol{\lambda}_d \tag{36}$$

$$\boldsymbol{\Delta}\bar{F} \triangleq \int_0^t \boldsymbol{\Delta}\bar{\lambda} d\boldsymbol{\vartheta} \tag{37}$$

4. SIMULATION

A simulation with a manipulator was carried out for illustration proposes. For the simulation a two–links planar manipulator with revolute joints was considered. The parameters used for the numerical simulation were: mass of the links, $m_1 = 3.9473$[Kg], $m_2 = 0.6232$[Kg], length of the links, $l_1 = l_2 = 0.38$[m], and viscous friction coefficients, $d_1 = d_2 = 1.2[\mathrm{N \cdot m/rad}]$. The task consisted on force and position tracking over a rigid surface considering both control approaches. The assumed surface is a segment of a circle described by

$$\varphi(\boldsymbol{x}) = (x-h)^2 + (y-k)^2 - r^2 = 0 \tag{38}$$

where (x, y) stands for the task-space coordinates, $r = 0.1[m]$ is the radius, and $(h, k) = (0.4, 0)[m]$ are the coordinates of the center of the circle. At the beginning of the task, the tip of the robot manipulator is in contact with the surface. The task consisted in following a trajectory from the point $(x, y) = (0.32, 0.06)[m]$ to the point $(x, y) = (0.48, 0.06)[m]$ over the surface in a time $t_f = 10[sec]$, while simultaneously it is desired to track a force signal given by (Gutiérrez-Giles and Arteaga-Pérez, 2016)

$$\lambda_d(t) = \begin{cases} 20 + 40(\cos(0.8\pi t/t_f)\sin(1.6\pi t/t_f))[\mathrm{N}] & \text{if } t \leq t_\mathrm{f} \\ 20 + 40(\cos(0.8\pi)\sin(1.6\pi))[\mathrm{N}] & \text{if } t > t_\mathrm{f} \end{cases} \tag{39}$$

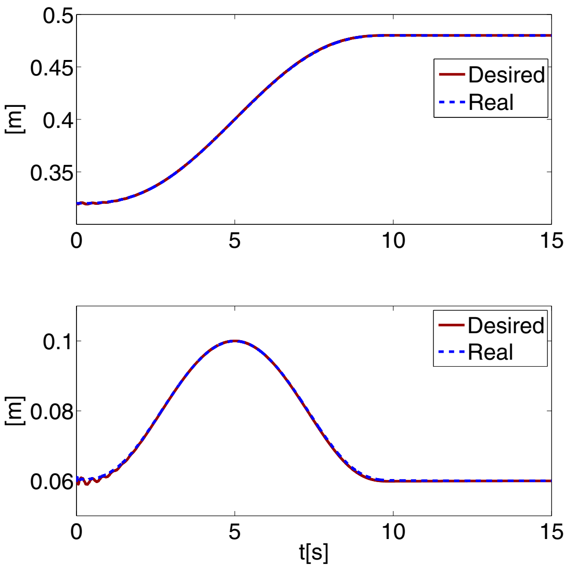

Fig. 2. Position tracking in Cartesian coordinates, *GPI* scheme.

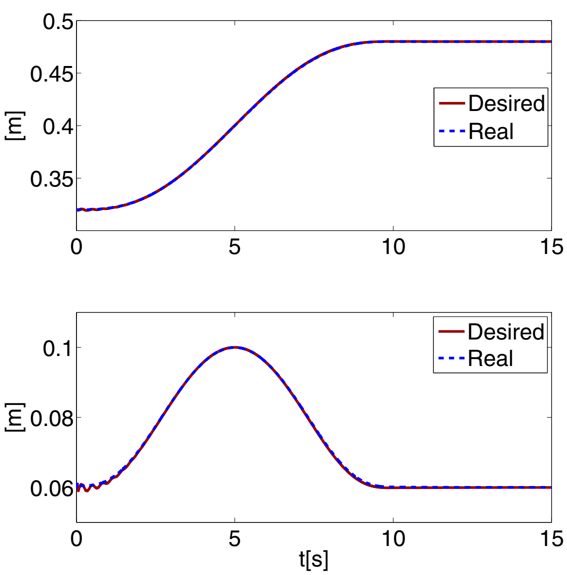

Fig. 3. Position tracking in Cartesian coordinates, *Levant* scheme.

The controller gains for the manipulator control law with the *GPI* scheme are $K_p = diag(1500; 1500)$, $K_v = diag(10; 10)$, $K_i = diag(1000; 1000)$, and $k_{Fi} = 0.5$, and for the *Levant* scheme are $K_p = diag(1850; 1850)$, $K_v = diag(10; 10)$, $K_i = diag(1000; 1000)$, and $k_{Fi} = 0.5$. The gains used for the GPI $\boldsymbol{K}_{\mathrm{v}} = \mathrm{diag}(10, 10)$, $\boldsymbol{\Lambda} = \mathrm{diag}(20, 20)$.

In Figure 2 and Figure 3 the position of the manipulator is shown in cartesian coordinates for both schemes. The velocity estimation with the GPI and the Levant differentiator is shown in Figure 4 and Figure 5. In this figures

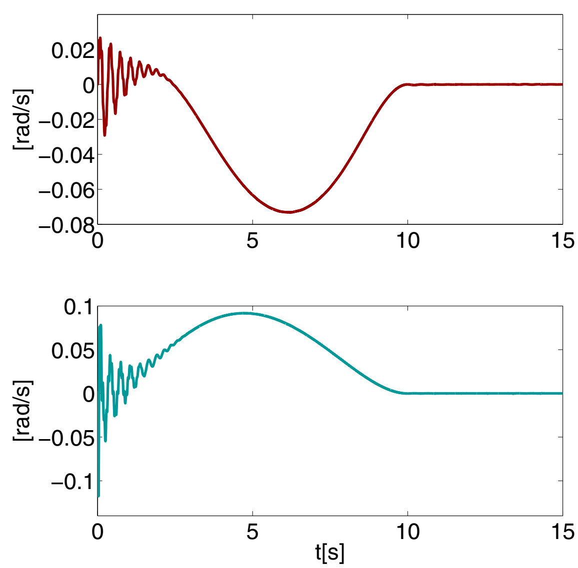

Fig. 4. Joint velocity manipulator, *GPI* scheme.

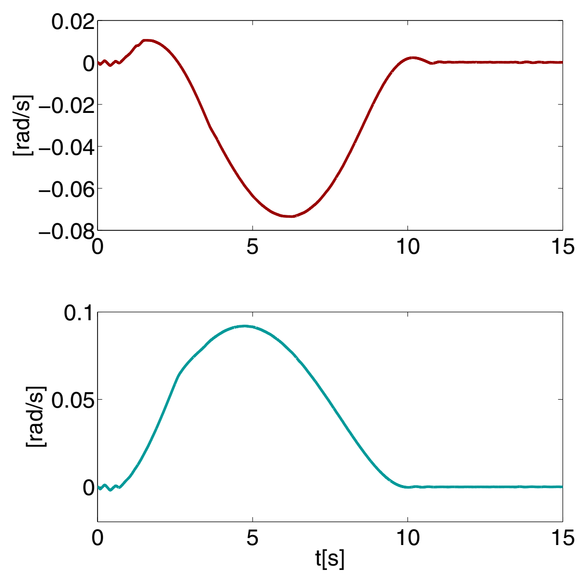

Fig. 5. Joint velocity manipulator, *Levant* scheme.

one can see that the estimation of the velocity is pretty accurate and converges in steady state. Figure 6 shows a velocity estimation comparison. The velocity estimation error is shown in Figure 7 and Figure 8. The position tracking and the tracking error in cartesian coordinates are shown in Figure 9 and Figure 10. Finally, Figures 11 and 12 show the position tracking in the xy plane.

5. CONCLUSIONS

In this work, a comparison between two velocity estimator schemes is considered, a observer design and a differentiator were presented. The latter proposed algorithm only

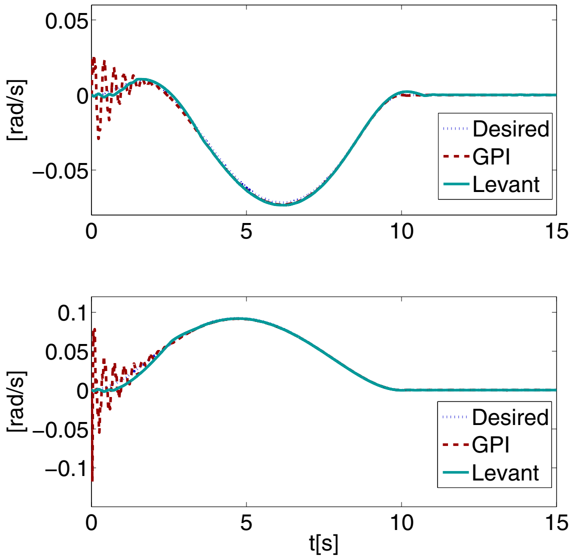

Fig. 6. Velocity estimation comparison.

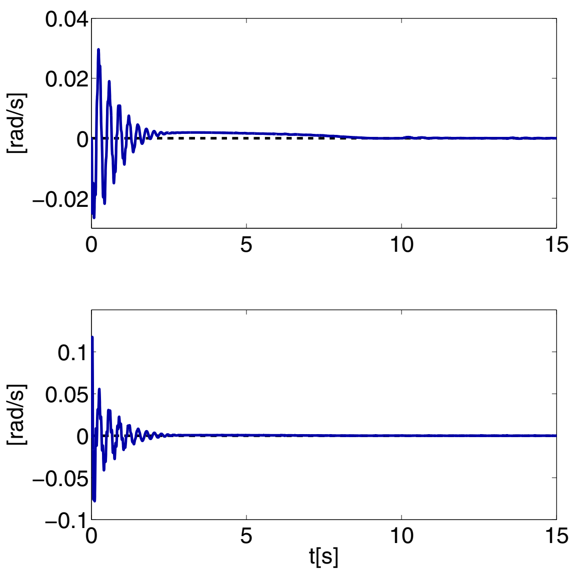

Fig. 7. Velocity estimation error, *GPI* scheme.

needs the measure of the joint position of the manipulator *i.e.,* it does not need the knowledge of the dynamic model. A numerical simulation was carried out to illustrate the effectiveness of the approach. So controller design becomes cheap and simpler. Simulation results were provided to demonstrate the efficacy of the approach. Two velocity estimator approaches were designed to obtain close tracking position over a rigid surface. As the simulation results show the good performance of the Levant differentiator approach. For implementation results, only one sensor is required for the measurement of position for each joint and velocity is estimated through Levant differentiator.

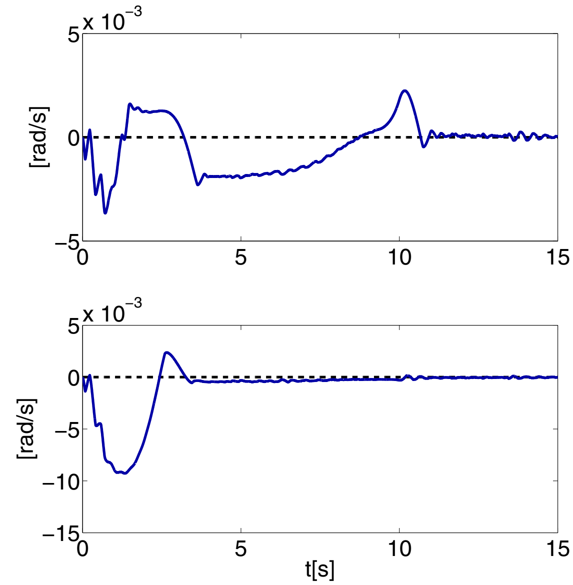

Fig. 8. Velocity estimation error, *Levant* scheme.

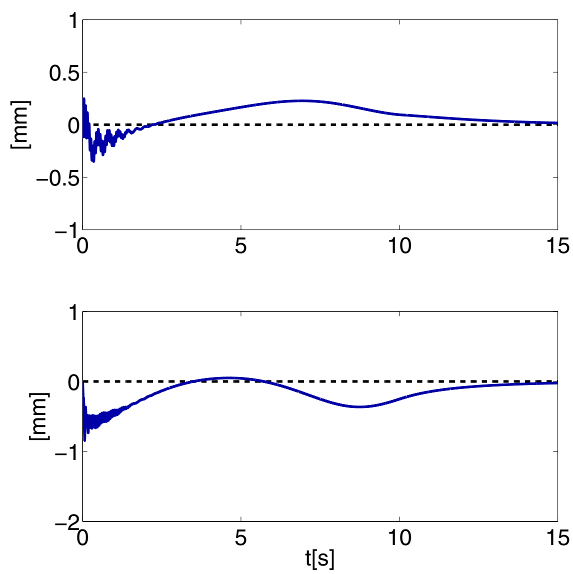

Fig. 9. Position tracking error, *GPI* scheme.

As a future work, it will be studied the suitability of the proposed approach in a experimental platform considering a master-slave teleoperation system interacting with a rigid surface in presence of friction.

ACKNOWLEDGEMENTS

This work is based on research supported by the **PAPIIT-UNAM** under grant No. **IN114617**.

REFERENCES

Arteaga-Pérez, M.A. (1998). On the properties of a dynamic model of flexible robot manipulators. *ASME*

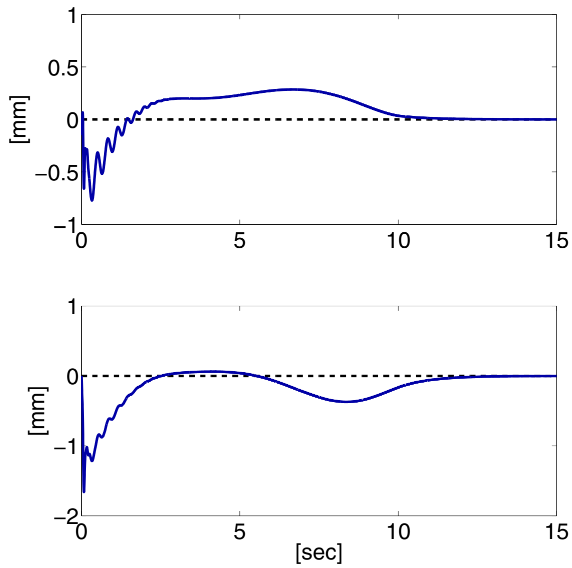

Fig. 10. Position tracking error, *Levant* scheme.

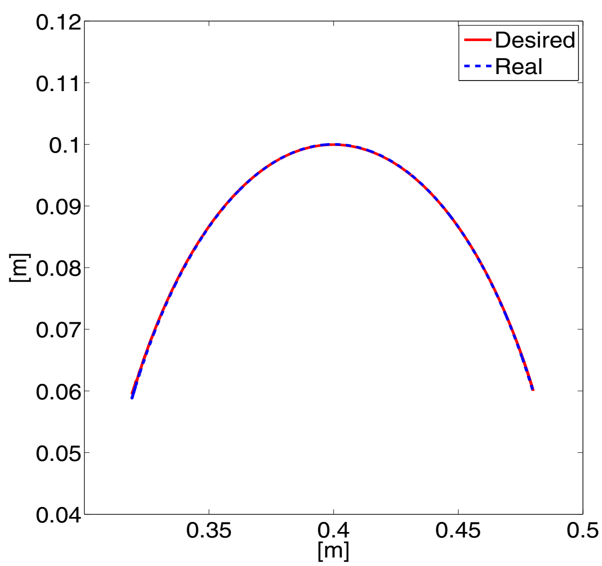

Fig. 11. Position tracking in the xy plane, *GPI* scheme.

Journal of Dynamic Systems, Measurement, and Control, 120, 8–14.

Arteaga-Pérez, M.A., Rivera-Dueñas, J.C., and Gutiérrez-Giles., A. (2013). Velocity and force observers for the control of robot manipulators. *Journal of Dynamic Systems, Measurement, and Control*, 135(6), 329–336.

Gutiérrez-Giles, A. and Arteaga-Pérez, M.A. (2016). Transparent bilateral teleoperation interacting with unknown remote surfaces with a force/velocity observer design. *International Journal of Control*, 1–27.

Gutiérrez-Giles, A. and Arteaga-Pérez, M.A. (2014). Gpi based velocity/force observer design for robot manipulators. *ISA transactions*, 53(4), 929–938.

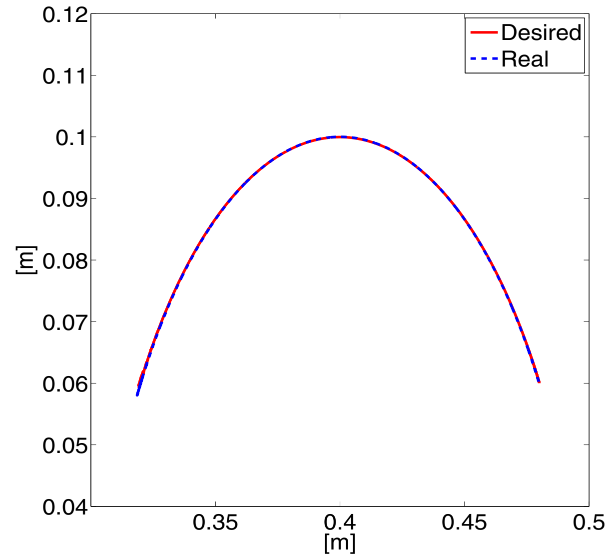

Fig. 12. Position tracking in the xy plane, *Levant* scheme.

Gutiérrez-Giles, I.A. (2016). *Transparent teleoperation with unknown surfaces and force estimation.* Master's thesis, UNIVERSIDAD NACIONAL AUTÓNOMA DE MÉXICO.

Hacksel, P. and Salcudean, S. (1994). Estimation of environment forces and rigid-body velocities using observers. *IEEE International Conference on, San Diego, CA*, vol.2 doi:10.1109/ROBOT.1994.351233., 931–936.

Jung, S. and Hsia, T.C. (2000). Robust neural force control scheme under uncertainties in robot dynamics and unknown environment. *IEEE Transactions on Industrial Electronics*, 47(2), 403–412. doi: 10.1109/41.836356.

Levant, A. (2003). Higher-order sliding modes, differentiation and output-feedback control. *International journal of Control*, 76(9–10):924–941. doi: 10.1109/9.362847.

Martínez-Rosas, J.C., Arteaga-Pérez, M.A., and Castillo-Sánchez., A. (2006). Decentralized control of cooperative robots without velocity-force measurements. *Automatica*, 42, 329–336.

Shaft, A.J.v.d. and Schumacher, H. (2000). An introduction to hybrd dynamical systems. *volume 251 of Lecture Notes in Control and Information Sciences. Springer 1 st edition.*

Shtessel, Y., Fridman, C.E.L., and Levant, A. (2014). *Sliding Mode control and Observation.* Springer.

Sira-Ramírez, H., Ramírez-Neria, M., and Rodríguez-Ángeles, A. (2010). On the linear control of nonlinear mechanical systems. 49th IEEE Conference on Decision and Control, Atlanta, GA, USA.